Inorganic Chemistry

ARTICLE

pubs.acs.org/IC

Strategy for the Rational Design of Asymmetric Triply Bridged Dinuclear 3d-4f Single-Molecule Magnets.

Enrique Colacio,*[,†] José Ruiz-Sanchez,[†] Fraser J. White,[‡] and Euan K. Brechin*[,‡]

[†]Departamento de Química Inorgánica, Facultad de Ciencias, Universidad de Granada, Av. Fuentenueva S/N, 18071 Granada, Spain

[‡]EaStCHEM School of Chemistry, The University of Edinburgh, West Mains Road, Edinburgh EH9 3JJ, United Kingdom

Supporting Information

ABSTRACT: Three triply bridged M^{II}-Dy^{III} dinuclear complexes, $[Ni(\mu\text{-L})(\mu\text{-OAc})Dy(NO_3)_2]$ **1**, $[Zn(\mu\text{-L})(\mu\text{-OAc})Dy(NO_3)_2]$ **2**, and $[Ni(\mu\text{-L})(\mu\text{-NO}_3)Dy(NO_3)_2]\cdot 2CH_3OH$ **3** were prepared with a new and flexible compartmental ligand, *N*,*N*′,*N*″-trimethyl-*N*,*N*″-bis(2-hydroxy-3-methoxy-5-methylbenzyl)diethylene triamine (H_2L), containing N_3O_2-inner and O_4-outer coordination sites. These complexes have diphenoxo/acetate (**1** and **2**) or diphenoxo/nitrate (**3**) asymmetric bridging fragments. Compounds **1** and **3** exhibit ferromagnetic interaction between Ni^{2+} and Dy^{3+} ions and frequency dependence of the out-of-phase (χ''_M) alternating current (ac) susceptibility signal characteristic of single-molecule-magnet behavior. The energy barriers Δ/k_B for compound **3** under zero and 1000 Oe applied direct current (dc) magnetic fields were estimated from the Arrhenius plots to be 7.6 and 19.1 K, respectively.

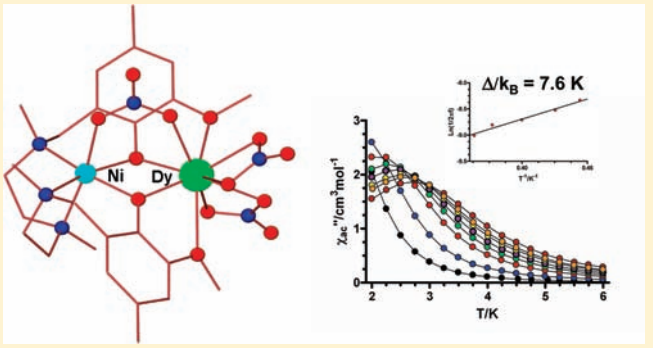

INTRODUCTION

The field of the Molecular Magnetism based on coordination compounds has experienced a renaissance in the two past decades with the discovery of molecular complexes that exhibit slow relaxation of the magnetization and magnetic hysteresis below the so-called blocking temperature (T_B) without undergoing three-dimensional (3D) magnetic ordering. These nanomagnets, called Single-Molecule Magnets (SMMs),[1,2] straddle the quantum/classical interface showing quantum effects such as quantum tunnelling of the magnetization and quantum phase interference. They are also potential candidates for magnetic information storage and quantum computing.[3] The origin of the SMM behavior is the existence of an energy barrier (Δ) that prevents reversal of the molecular magnetization and causes slow relaxation of the magnetization at low temperature. This energy barrier depends on the large-spin multiplicity of the ground state (S_T) and the easy-axis (or Ising-type) magnetic anisotropy of the entire molecule ($D < 0$). The early examples of SMMs were clusters of transition metal ions,[1] the majority being Mn clusters containing at least some Mn^{III} centers, but recently mixed 3d/4f metal aggregates[2] and even low-nuclearity 4f metal complexes[4] have been shown to possess SMM behavior. The reasons why heavy lanthanide ions (Dy^{III}, Tb^{III}, Ho^{III}, and Er^{III}) have been used to design SMMs are 3-fold: (i) they have large angular moments, and large magnetic moments, in the ground multiplet state, as a consequence of strong spin−orbit coupling; (ii) the symmetry of the ligand field around the lanthanide ion may lead to ground-state doublets with large $|M_J|$ values, thus achieving an easy axis of the magnetization and large Ising-type magnetic anisotropy; (iii) the magnetic coupling of the heavy lanthanide with the 3d transition metal ions is often ferromagnetic, which leads to ground states with even larger magnetic moments.

Many of the original 3d-4f systems exhibiting SMM behavior were prepared using Schiff base ligands, which were synthesized from o-vanillin and different diamines. These ligands are of two general types: compartmental[2b,5] and tripodal.[6] The former have two different coordination sites; the inner site (commonly of the N_4O_2 type) showing preference for transition metal ions and the outer site (O_4) showing preference for hard, oxophilic metal ions such as lanthanides. Compartmental ligands therefore usually give rise to dinuclear M-Ln systems. To fully saturate the coordination sphere of the transition and lanthanide metal ions, solvent molecules are usually coordinated to the former ion and anions to the latter. The solvent molecules can be replaced by donor atoms belonging to either a bridging ligand or a complex acting as bridging ligand to afford materials exhibiting increased nuclearity and dimensionality based on connected 3d-4f units.[2b] These Schiff base compartmental ligands are rather rigid and afford almost planar 3d-4f systems. The lack of flexibility of this type of ligand also prevents the coordination of ions with different ionic radii such as Mn^{II} and Zn^{II} in the inner site. Tripodal ligands possess a fully saturated N_3O_3 inner site and an O_6 outer site, and generally yield M-Ln-M trinuclear systems.

Received: April 24, 2011
Published: June 29, 2011

Scheme 1. Ligand H_2L and Its Coordination Sites

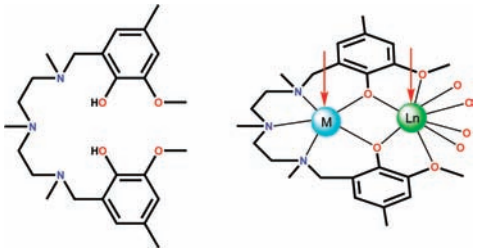

Because the coordination sphere of the transition metal ions occupying the inner site is saturated, in principle, no further reactions are possible with additional bridging ligands.

To overcome the drawbacks of the Schiff-base compartmental ligands and to enhance their positive features, we have designed a new ligand (H_2L= *N*,*N*′,*N*″-trimethyl-*N*,*N*″-bis(2-hydroxy-3-methoxy-5-methylbenzyl)diethylene triamine, see Scheme 1) that presents the following advantages: (i) the absence of double imine bonds confers greater flexibility, allowing the coordination of transition metal ions with rather different sizes in the inner site. Therefore, a large variety of 3d-4f combinations can be obtained. (ii) The N_3O_2 pentacoordinated inner site forces the metal ions with high preference for octahedral coordination to saturate their coordination sphere with a donor atom (note that in the case of Ni^{II}, a paramagnetic species will always be obtained), which can proceed from a bridging ligand connecting the Ln and the transition metal ions. If so, novel triply bridged 3d-4f complexes could be obtained. (iii) The ligand does not contain active hydrogen atoms that would promote intermolecular hydrogen bonds thus allowing the formation of well isolated molecules in crystal lattice, favoring SMM behavior.

In this paper we report the synthesis, X-ray structures, and magnetic properties of three triply bridged M^{II}-Dy^{III} dinuclear complexes, $[Ni(\mu\text{-L})(\mu\text{-OAc})Dy(NO_3)_2]$ **1**, $[Zn(\mu\text{-L})(\mu\text{-OAc})Dy(NO_3)_2]$ **2**, and $[Ni(\mu\text{-L})(\mu\text{-NO}_3)Dy(NO_3)_2]\cdot 2CH_3OH$ **3** having $Ni(\mu\text{-diphenoxo})(\mu\text{-X})Dy$ (X = *syn-syn* OAc^- or NO_3^-) bridging fragments. Compounds **1** and **3** represent rare examples of dinuclear Ni^{II}—Dy^{III} complexes exhibiting SMM behavior. Although Dy-containing compounds often exhibit SMM behavior, there are as yet no examples of dinuclear Ni—Dy SMMs.

EXPERIMENTAL SECTION

General Procedures. Unless stated otherwise, all reactions were conducted in oven-dried glassware in aerobic conditions, with the reagents purchased commercially and used without further purification.

Synthesis of H_2L. The ligand H_2L was prepared by refluxing a solution of *N*,*N*′,*N*″-trimethylethylenediamine (5.81 g, 40 mmol), 2-methoxy-4-methyl-phenol (11.04 g, 80 mmol), and 37% paraformaldehyde (6.28 g, 80 mmol) in MeOH (150 mL) during 8 h. After cooling to room temperature, white needles were obtained, which were filtered off, washed with cool methanol, and diethylether and air-dried. Yield: 67%. Anal. Calcd. for $C_{25}H_{39}N_3O_4$: C, 67.37; H, 8.83; N, 9.43. Found: C, 67.21; H, 9.05; N, 9.32; IR (KBr, cm^{-1}): 3053 (s), 3006 (s), 2953 (vs), 2834 (vs), 2734 (s), 1590 (s), 1499 (vs), 1091 (m), 830 (m), 827 (m), 783 (m). ^{1}**H NMR** (400 MHz, (CD_3Cl) δ 6.58 (2H, s, C_4-**H**, C_4'-**H**), 6.37 (2H, s, C_6-**H**, C_6'-H), 3.82(6H, s, OCH_3), 3.62 (4H, s, N−CH_2-C1), 2.55−2.61 (8H, m, N−CH_2-CH_2−N-CH_2CH_2-N), 2.25 (6H, s, -C_5−CH_3), 2.21 (9H, s, N−CH_3); ^{13}**C NMR** (101 MHz, (CD_3Cl) δ 147.9 (C_3-H, C_3'-H), 144.9 (C_2−OH, C_2'−OH), 128.11 (C_5-CH_3, C_5'-CH_3), 122.1 (C_1-CH_2−, C_1'-CH_2−), 121.3 (C_6-H, C_6'-H), 112.3 (C_4-H, C_4'-H), 60.8 (C_1-CH_2-, C_1'-CH_2-), 56.1 (OCH_3), 55.5 (N-CH_2−CH_2−N-CH_2CH_2−N), 54.7 (N−CH_2-CH_2−N-CH_2CH_2−N), 42.5 (N′-CH_3), 42.1 (N-CH_3, N″-CH_3), 21.2 (C_5-CH_3).

Preparation of Complexes (1)−(3). *$[Ni(\mu\text{-L})(\mu\text{-Ac})Dy(NO_3)_2]$ (**1**).* To a solution of H_2L (55.7 mg, 0.125 mmol) in 5 mL of MeOH were subsequently added with continuous stirring 31.1 mg (0.125 mmol) of $Ni(Ac)_2\cdot 4H_2O$ and 54.8 mg (0.125 mmol) of $Dy(NO_3)_3\cdot 5H_2O$. The resulting pale green solution was filtered and allowed to stand at room temperature. After 1 day, well formed prismatic light blue crystals of compound **1** were obtained. Yield: 70%. IR (KBr, cm^{-1}): 2981 (m), 2915 (m), 2864 (m), 1576 (s), 1494 (vs), 1384 (s), 1300 (s), 1080 (m), 1070 (m), 815 (m), 795 (m), 619 (m). Anal. Calcd. for $C_{27}H_{40}N_5O_{12}$-NiDy: C, 38.23; H, 4.76; N, 8.26. Found: C, 38.10; H, 4.55; N, 8.32.

*$[Zn(\mu\text{-L})(\mu\text{-Ac})Dy(NO_3)_2]$ (**2**).* This compound was prepared in a 60% yield as colorless crystals following the same procedure as for **1**, but using $Zn(Ac)_2\cdot 2H_2O$ (27.4 mg, 0.125 mmol) instead of $Ni(Ac)_2\cdot 4H_2O$. IR (KBr, cm^{-1}): 2975 (m), 2918 (m), 2866 (m), 1578 (s), 1494 (vs), 1384 (s), 1301 (s) 1080 (m), 1071 (m), 813 (m), 794 (m), 619 (m). Anal. Calcd. for $C_{27}H_{40}N_5O_{12}ZnDy$: C, 37.93; H, 4.72; N, 8.20. Found: C, 37.90; H, 4.67; N, 8.37.

*$[Ni(\mu\text{-L})(\mu\text{-NO}_3)Dy(NO_3)_2]\cdot 2CH_3OH$ (**3**).* This compound was prepared in a 65% yield as light blue crystals following the procedure for **1**, except that $Ni(NO_3)_2\cdot 6H_2O$ (54.8 mg, 0.125 mmol) was used instead of $Ni(Ac)_2\cdot 4H_2O$. IR (KBr, cm^{-1}): 2920 (m), 1469 (s), 1384 (vs), 1311 (m), 1254 (m), 1088 (m), 815 (m). Anal. Calcd. for $C_{27}H_{45}N_6O_{15}$-NiDy: C, 35.43; H, 4.96; N, 9.19. Found: C, 35.21; H, 5.05; N, 9.32.

Physical Measurements. Elemental analyses were carried out at the "Centro de Instrumentación Científica" (University of Granada) on a Fisons-Carlo Erba analyzer model EA 1108. The IR spectra on powdered samples were recorded with a ThermoNicolet IR200FTIR by using KBr pellets. Magnetization and variable temperature (2−300 K) magnetic susceptibility measurements on polycrystalline samples were carried out with a Quantum Design SQUID MPMS XL-5 device operating at different magnetic fields. The experimental susceptibilities were corrected for the diamagnetism of the constituent atoms by using Pascal's tables.

Single-Crystal Structure Determination. Suitable crystals of **1**−**3** were mounted on glass fiber and used for data collection. Data were collected with a dual source Oxford Diffraction SuperNova diffractometer equipped with an Atlas CCD detector and an Oxford Cryosystems low temperature device operating at 100 K and using Mo-K_α. Semiempirical (multiscan) absorption corrections were applied using Crysalis Pro.[7] The structures were solved by direct methods[8] and refined with full-matrix least-squares calculations on F^2.[9] Anisotropic temperature factors were assigned to all atoms except for the hydrogens, which are riding their parent atoms with an isotropic temperature factor arbitrarily chosen as 1.2 times that of the respective parent. Final $R(F)$, $wR(F^2)$, and goodness of fit agreement factors, details on the data collection, and analysis can be found in Table 1. Selected bond lengths and angles are given in Supporting Information, Table S1.

RESULTS AND DISCUSSION

The reaction of H_2L with either $Ni(OAc)_2\cdot 4H_2O$ or $Zn(OAc)_2\cdot 2H_2O$ and subsequently with $Dy(NO_3)_3\cdot 6H_2O$ in MeOH in 1:1:1 molar ratio led to light blue crystals of the compound $[Ni(\mu\text{-L})(\mu\text{-OAc})Dy(NO_3)_2]$ (**1**) and colorless crystals of the compound $[Zn(\mu\text{-L})(\mu\text{-OAc})Dy(NO_3)_2]$ (**2**), respectively. The same reaction but using $Ni(NO_3)_3\cdot 6H_2O$ instead of $Ni(OAc)_2\cdot 4H_2O$ afforded light blue crystals of the compound $[Ni(\mu\text{-L})(\mu\text{-NO}_3)Dy(NO_3)_2]\cdot 2CH_3OH$ (**3**). Compounds **1** and **2** are isostructural (the structure of **1** is given in Figure 1 as an example) and their structures consist of two almost

dx.doi.org/10.1021/ic2008599 |*Inorg. Chem.* 2011, 50, 7268–7273

Table 1. Crystallographic Data for Complexes 1−3

	1	2	3
formula	$C_{27}H_{40}N_5O_{12}DyNi$	$C_{27}H_{40}N_5O_{12}DyZn$	$C_{27}H_{45}N_6O_{15}DyNi$
M_r	847.85	854.51	914.90
crystal system	triclinic	triclinic	monoclinic
space group (no.)	$P\bar{1}$ (2)	$P\bar{1}$ (2)	$P2_1/c$ (14)
a (Å)	11.39980(16)	11.44727(16))	10.5754(3
b (Å)	14.7243(2)	14.7621(2)	21.0771(5)
c (Å)	19.4119(3)	19.3317(3)	16.4485(4)
α (deg)	92.3970(12)	92.6188(11)	90
β (deg)	98.2700(12)	98.4920(11)	105.4010(10)
γ (deg)	91.0070(11)	90.9853(11)	90
V (Å^3)	3220.74(8)	3226.64(8)	3534.69(16)
Z	4	4	4
D_c (g cm^{-1})	1.749	1.759	1.719
μ(MoK$_\alpha$) (mm^{-1})	2.955	3.110	2.706
T/K	100 (2)	100(2)	100(2)
observed reflections	16085 (12880)	16339(14322)	7050(6070)
R_{int}	0.0473	0.0357	0.0331
parameters	845	845	462
GOF on F^2	1.085	1.119	1.033
R_1[a]	0.0476(0.0350)[b]	0.0293(0.0241)	0.0325(0.0246)
wR_2[c]	0.0792(0.0770)	0.0611(0.0592)	0.0552(0.0526)
largest difference in peak and hole (e Å^{-3})	5.480 and −2.531	1.427 and −1.097	0.660 and −0.694

[a] $R_1 = \Sigma||F_o| - |F_c||/\Sigma|F_o|$. [b] Values in parentheses for reflections with $I > 2\sigma(I)$. [c] $wR_2 = \{\Sigma w(F_o^2 - F_c^2)^2/\Sigma w(F_o^2)^2\}^{1/2}$.

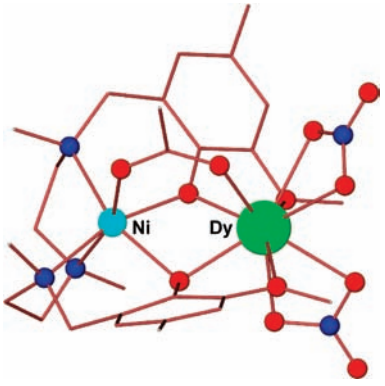

Figure 1. Perspective view of one of the crystallographically independent molecules of complex **1** . Color code: N = light blue, O = red, Ni = blue, Dy = green.

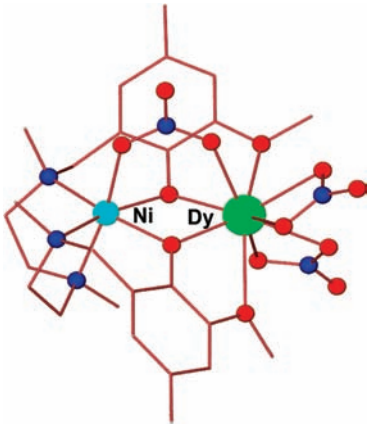

Figure 2. Perspective view of the molecular structure of complex **3**. Color code: N = light blue, O = red, Ni = blue, Dy = green.

identical dinuclear M^{II}-Dy^{III} molecules, in which the Dy^{III} and M^{II} ions (M = Ni and Zn) are bridged by two phenoxo groups of the L^{2-} ligand and one *syn-syn* acetate anion.

The L^{2-} ligand wraps around the Ni^{II} ions in such a way that the three nitrogen atoms, and consequently the three oxygen atoms, occupy *fac* positions on the slightly trigonally distorted NiN_3O_3 coordination polyhedron. The Dy^{3+} ion exhibits a DyO_9 coordination sphere which is made by the two phenoxo bridging oxygen atoms, the two methoxy oxygen atoms, one oxygen atom from the acetate bridging group, and four oxygen atoms belonging to two bidentate nitrate anions. The average Dy−O distances are in the range 2.22 Å−2.68 Å for **1** and 2.22 Å−2.73 Å for **2**, thus indicating a high degree of asymmetry in the DyO_9 coordination sphere. In fact, the calculation of the degree of distortion of the Dy coordination polyhedron with respect to ideal nine-vertex, by using the continuous shape measure theory and SHAPE software,[10] led to shape measures relative to the, muffin (C_s), spherical capped square antiprism (C_{4v}), spherical tricapped trigonal prism (D_{3h}) and capped square-antiprims (C_{4v}) with values of 2.24, 2.35, 2.99, and 3.14, respectively, for **1** and 2.26, 2.28, 3.01, and 3.24, respectively, for **2**. Therefore, the DyO_9 coordination sphere can be considered as intermediate between all theses nine-vertex polyhedra. The shape measures relative to other reference polyhedra are significantly larger. The bridging fragment is also rather asymmetric with different bond angles and distances involving the Dysprosium and transition metal ions. The average Dy−O−M angles are 101.37° and

dx.doi.org/10.1021/ic2008599 |*Inorg. Chem.* 2011, 50, 7268–7273

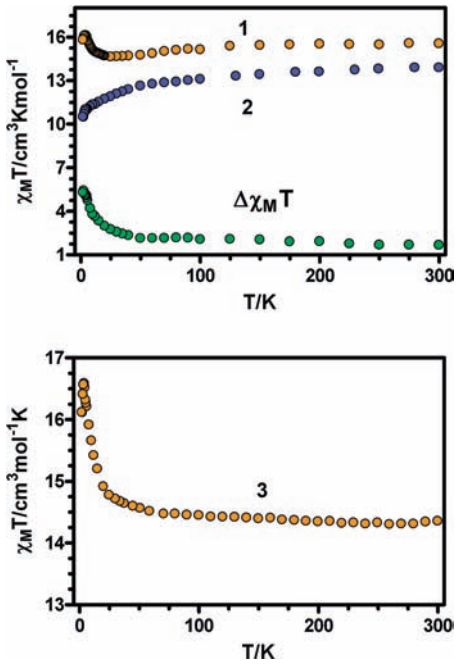

Figure 3. Temperature dependence of the $\chi_M T$ product for **1**, **2** and the difference $\Delta\chi_M T = (\chi_M T)_{NiDy} - (\chi_M T)_{ZnDy} = (\chi_M T)_{Ni} + J_{NiDy}(T)$ (top), and temperature dependence of the $\chi_M T$ product for **3** (bottom).

107.35° for **1** and 100.92° and 107.04° for **2**. The bridging acetate group forces the structure to be folded with the average hinge angle of the M(μ-O_2)Dy bridging fragment being 21.30° for **1** and 23.50° for **2**. The intradinuclear Ni−Dy and Zn−Dy distance are 3.42 Å and 3.45 Å, respectively.

Complex **3** possess a molecular structure very similar to that of **1** but having a bridging nitrate anion connecting the Dy^{III} and Ni^{II} metal ions instead of an acetate anion (Figure 2). The coordination of the nitrato bridging ligand induces a higher planarity on the Ni(μ-O_2)Dy bridging fragment of the structure. Thus, the hinge angle decreases to a value of approximately 13° with a concomitant decrease of the out-of-plane displacements of the O−C bonds belonging to the phenoxo bridging groups from the $Ni(O)_2Ni$ plane. Bond distances are almost identical for **1** and **3** with the exception of the Ni−O and Dy−O bond distances involving the oxygen atoms of the bridging anion, which increase on going from acetate to nitrate by approximately 0.1 Å. Notice that the computed shape measures relative to the ideal six-vertex and nine-vertex polyhedra, for the NiN_3O_3 and DyO_9 coordination polyhedra, respectively, were very close to those obtained for compound **1**. In particular, the shape measures for the DyO_9 coordination polyhedra relative to the spherical capped square antiprism (C_{4v}), muffin (C_s) capped square-antiprims (C_{4v}) and spherical tricapped trigonal prism (D_{3h}) were of 1.78, 1.80, 2.24, and 2.25, respectively.

Finally, it should be stressed that none of these compounds exhibit interdinuclear hydrogen bond interactions.

The magnetic susceptibilities of complexes **1**−**3** have been measured in the 2−300 K temperature range under an applied magnetic field of 0.1 T (Figure 3).

The $\chi_M T$ value of 15.53 cm^3 K mol^{-1} at 300 K for **1** (Figure 3, top) is compatible with the calculated value of 15.17 cm^3 K mol^{-1} for independent Ni^{II} ($S = 1$) and Dy^{III} ($4f^9$, $J = 15/2$, $S = 5/2$, $L = 5$, $^6H_{15/2}$) in the free-ion approximation. The $\chi_M T$ value

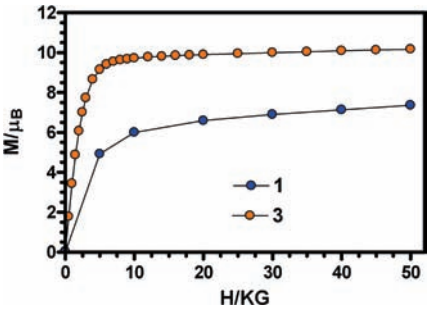

Figure 4. *M* versus *H* plots for **1** and **2** at 2 K. Solid lines are a guide to the eye.

decreases slowly with decreasing temperature down to a minimum value of 14.64 cm^3 K mol^{-1} at 25.0 K, then increases at lower temperatures, reaching a maximum value of 16.0 cm^3 K mol^{-1} at 5 K. Below this temperature, the $\chi_M T$ value drops abruptly. The slight decrease of the $\chi_M T$ product between 300 and 25 K is due to the depopulation of the Stark sublevels of the dysprosium ion, which arise from the splitting of the $^6H_{15/2}$ ground term by the ligand field and whose width is on the order of 100 cm^{-1}. The increase of $\chi_M T$ below 25 K is likely to be due to a ferromagnetic interaction between Ni^{II} and Dy^{III}, whereas the decrease of $\chi_M T$ below 5 K is probably associated with the presence of magnetic anisotropy and/or weak antiferromagnetic interactions between the dinuclear complexes. To unequivocally know the nature of the magnetic interaction between Ni^{II} and Dy^{III}, the empirical approach developed by Costes et al.[11] was applied. In this approach, the contribution of the crystal-field effects of the Dy^{3+} ion is removed by subtracting from the experimental $\chi_M T$ data of **1** those of the isostructural complex **2**, whose magnetic behavior depends only on the Dy^{3+} ion. The difference $\Delta\chi_M T = (\chi_M T)_{NiDy} - (\chi_M T)_{ZnDy} = (\chi_M T)_{Ni} + J_{NiDy}$ is therefore related to the nature of the overall exchange interaction between the Ni^{II} and Dy^{III} ions. Thus, positive values are related to ferromagnetic couplings whereas negative values are related to antiferromagnetic interactions. The $\Delta\chi_M T$ value is almost constant over the whole temperature range, except for an increase in the lowest-temperature region, thus indicating a ferromagnetic interaction between Ni^{II} and Dy^{III} ions.

The thermal variation of the $\chi_M T$ product for **3** at 1000 Oe is given in Figure 3. The value at 300 K (14.3 cm^3 K mol^{-1}) is not far from that expected, 15.17 cm^3 K mol^{-1}. The $\chi_M T$ product increases continuously with decreasing temperature to reach a maximum at 4 K (16.6 cm^3 K mol^{-1}) and then shows a sharp decrease down to 2 K to a value of 16.1 cm^3 K mol^{-1}. It seems that the effect of depopulation of the Stark sublevels in **3** is not as pronounced as in **1**. The increase in the $\chi_M T$ product between 300 and 4 K for **3** supports the existence of a ferromagnetic exchange interaction between the Ni^{II} and Dy^{III} ions through the phenoxo and nitrate bridging groups.

The field dependence of the magnetization at 2 K for **1** (Figure 4) reveals a relatively slow increase of the magnetization at low fields and then a linear increase without clear saturation above 4 T. The magnetization at 7 T is 7.56 μ_B. The linear high-field variation of the magnetization suggests the presence of a significant magnetic anisotropy and/or low-lying excited states that are partially [thermally and field-induced] populated. These low-lying excited states are in agreement with weak magnetic interactions expected for 3d-4f systems. The *M* versus *H* plot

dx.doi.org/10.1021/ic2008599 |*Inorg. Chem.* 2011, 50, 7268–7273

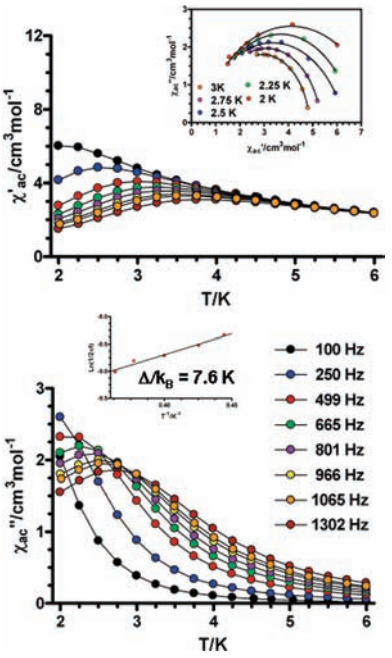

Figure 5. Temperature dependence of in-phase χ'_M (top) and out-of-phase χ''_M (bottom) components of the alternating current (ac) susceptibility for complex **3** measured under zero applied dc field. Top inset: Cole−Cole (Argand) plot of χ'_M versus χ''_M in the 2.0−3.0 K temperature range, in zero applied dc field, for compound **2**. The solid lines represent the best fit of the data to a generalized Debye model. Bottom inset: Relaxation time of the magnetization $\ln(2\pi f)$ versus T^{-1}, Arrhenius plot, for **2** . The solid line corresponds to the fit.

at 2 K for **3** (Figure 4) shows a relatively rapid increase in the magnetization at low field in accord with a high-spin state for this complex and a rapid saturation of the magnetization that is almost complete above 3 T, reaching a value of 10.2 μ_B. This behavior suggests the existence of a well-defined ground state that is stabilized by sufficiently large Ni−Dy magnetic interactions. In fact, the magnetization saturation value for **3** is close to that expected (11.2 μ_B) for a Dy^{3+} that has a strong easy-axis anisotropy, and behaves as an Ising spin at low temperatures with a $J_z = 15/2$, ferromagnetically coupled with the $S = 1$ value for the Ni^{2+} ion.[12]

The existence of a larger magnetic coupling for **3** than for **1** is not unexpected in view of the theoretical and experimental studies carried out on related dinuclear Cu-O_2-Gd complexes, which have shown that, for similar Cu−O−Gd bridging angles, there is a correlation between the magnitude of magnetic exchange coupling, J, and the dihedral angle between the two halves of the Cu-O_2-Gd bridging core: the larger the planarity of the Cu-O_2-Gd bridging core, the stronger is the ferromagnetic interaction.[13] If we assume that the same correlation applies for Ni-O_2-Dy complexes, then the magnetic exchange coupling between Ni^{II} and Dy^{III} for **3** should be higher than for **1** because the hinge angle for the former is smaller. Unfortunately, the magnetic properties of **1** and **3** can not be quantitatively analyzed because of the presence of spin−orbit coupling and crystal field effects.

Dynamic magnetic susceptibility measurements performed on these complexes clearly show the frequency dependency of the in-phase (χ'_M) and out-of-phase (χ''_M) signals. This behavior indicates the slow relaxation of the magnetization typical of a SMM. For **1**, (Supporting Information, Figure S1) the χ''_M signal is quite weak with a χ''_M/χ'_M ratio of only 0.05 and no maximum observed above 2 K at frequencies reaching 1300 Hz. Compound **3**, however, shows typical SMM behavior below 5 K (Figure 5). From the temperatures and frequencies of the maxima observed for the χ''_M signals, and by using an Arrhenius plot ($\tau = \tau_0 \exp(\Delta/k_BT)$, the energy barrier for the flipping of the magnetization was estimated to be 7.6 K with a pre-exponential factor $\tau_0 = 7.2 \times 10^{-6}$ s. The value of Δ/k_B is at the lower end of the experimental range found for similar 3d/4f SMM systems.[6a] The graphical representation of χ_M'' versus χ_M' (Cole−Cole plot[14]) in the temperature range 2.0−3.0 K is shown in the inset of Figure 5. The data were simulated using the conventional generalized Debye model, taking into account the width of the τ distribution by means of the α parameter ($0 < \alpha < 1$, the simple Debye model corresponding to $\alpha = 0$). The fit to the data affords α values in the range 0.25 (2 K) to 0.05 (at 3 K), suggesting multiple relaxation processes. When an external direct current (dc) magnetic field of 1000 Oe was applied, the quantum pathway of relaxation is fully or partly suppressed, and the frequency-dependent maxima in the χ''_M versus T plot are shifted to higher temperatures (Supporting Information, Figure S2). As expected the thermally activated barrier energy increases to a value of 19.1 K ($\tau_0 = 7.2 \times 10^{-7}$ s). Differences in the ligand crystal field around the Dy^{III} ions in **1** and **3**, and consequently in the local magnetic anisotropy, as well as the larger ferromagnetic interaction expected for **3**, leading to a more isolated ground state, may be responsible for the higher energy barrier observed for **3**.

In summary, we have designed a new type of compartmental ligand, with high backbone flexibility and a N_3O_2 inner coordination site, specifically adapted to form novel triply bridged [M(μ-L)(μ-X)Ln] dinuclear complexes. The validity of this strategy has been demonstrated with the preparation of M^{II}-Dy^{III} complexes (M^{II} = Ni and Zn) containing either diphenoxo/acetate (**1** and **2**) or diphenoxo/nitrate (**3**) bridging groups. Complexes **1** and **3** exhibit ferromagnetic interaction between Ni^{2+} and Dy^{3+} ions and frequency dependence of the out-of-phase (χ''_M) signal characteristic of SMMs. In particular, complex **3** represents the first example of a simple Ni−Dy dinuclear system exhibiting SMM behavior with a maximum in the out-of-phase (χ''_M) versus T plot above 2 K.[6b] We are now pursuing the completion of the series of complexes [M(μ-L)-(μ-X)Ln$(NO_3)_2$] as well as [Ln{M(μ-L)(μ-X)}$_2$Ln](NO_3) [(M^{II} = Mn, Fe, Co, Ni, Zn and Cu and Ln^{III} = Gd, Dy, Tb, Ho, and Er) with different X bridging groups, including anisotropic metal complexes acting as ligands, such as metal-cyanide and metal-chloride building blocks. We expect to obtain a large variety 3d-4f, 3d-4f-3d′, 3d-4f-4d(5d) complexes exhibiting SMM behavior with higher thermal energy barriers.

■ ASSOCIATED CONTENT

Supporting Information. Crystallographic data in CIF format, Figures S1−S2 and Table S1. This material is available free of charge via the Internet at http://pubs.acs.org.

■ AUTHOR INFORMATION

Corresponding Author

*E-mail: ecolacio@ugr.es (E.C.), ebrechin@staffmail.ed.ac.uk (E.K.B.).

■ ACKNOWLEDGMENT

This work was supported by the MEC (Spain) (Project CTQ-2008-02269/BQU), the Junta de Andalucía (FQM-195 and Project of excellence P08-FQM-03705), and the University of Granada. Financial support from the University of Granada and Junta de Andalucia for the visit of E.C. to the University of Edinburgh is grateful acknowledged. E.K.B. would like to thank the EPSRC and Leverhulme Trust for financial support. We would like to thank Dr. Antonio J. Mota, University of Granada, Spain, for his generous assistance with the SHAPE calculations

■ REFERENCES

(1) For some recent reviews see: (a) Gatteschi, D.; Sessoli, R. *Angew. Chem., Int. Ed.* **2003**, *42*, 268. (b) Christou, G. *Polyhedron* **2005**, *24*, 2065.(c) Gatteschi, D.; Sessoli, R.; Villain, J. *Molecular Nanomagnets*; Oxford University Press: Oxford, U.K., 2006. (d) Aromí, G.; Brechin, E. K. *Struct. Bonding (Berlin)* **2006**, *122*, 1. (e) Rebilly, J.-N.; Mallah, T. *Struct. Bonding (Berlin)* **2006**, *122*, 103. (f) Cornia, A.; Costantino, A. F.; Zobbi, L.; Caneschi, A.; Gatteschi, D.; Mannini, M.; Sessoli, R. *Struct. Bonding (Berlin)* **2006**, *122*, 133. (g) Milios, C. J.; Piligkos, S.; Brechin, E. K. *Dalton Trans.* **2008**, 1809.(h) Molecular Magnets", themed issue; Brechin, E. K., Ed.; *Dalton Trans.*, **2010** (i) Bagai, R.; Christou, G. *Chem. Soc. Rev.* **2009**, *38*, 1011.

(2) For some recent reviews see: (a) Sessoli, R.; Powell, A. K. *Coord. Chem. Rev.* **2009**, *253*, 2328. (b) Andruh, M.; Costes, J. P.; Diaz, C.; Gao, S. *Inorg. Chem.* **2009**, *48*, 3342, Forum Article.

(3) (a) Wernsdorfer., W.; Sessoli, R. *Science* **1999**, *284*, 133. (b) Leuenberger, M. N.; Loss, D. *Nature* **2001**, *410*, 789. (c) Meier, F.; Loss, D. *Phys. B* **2003**, *329*, 1140.

(4) See for instance: (a) Ishikawa, N.; Sugita, M.; Ishikawa, T.; Koshihara, S.-Y.; Kaizu, I. *J. Am. Chem. Soc.* **2003**, *125*, 8694. (b) Ishikawa, N.; Sugita, M.; Wernsdorfer, W. *Angew. Chem., Int. Ed.* **2005**, *44*, 2931. (c) AlDamen, M. A.; Cardona-Serra, S.; Clemente-Juan, J. M.; Coronado, E.; Gaita-Ariño, A.; Martí-Gastaldo, C.; Luis, F.; Montero, O. *Inorg. Chem.* **2009**, *48*, 3467, Forum Article. (d) Lin, P.-H.; Burchell, T. J.; Ungur, L.; Chibotaru, L. F.; Wernsdorfer, W.; Murugesu, M. *Angew. Chem., Int. Ed.* **2009**, *48*, 1 and references therein. (e) Abbas, G.; Lan, Y.; Kostakis, G. E.; Wernsdorfer, W.; Anson, C. E.; Powell, A. K. *Inorg. Chem.* **2010**, *49*, 8067 and references therein. Guo, Y.-N.; Xu, G.-F.; Gamez, P.; Zhao, L.; Lin, S.-Y.; Deng, R.; Tang, J.; Zhang, H.-J. *J. Am. Chem. Soc.* **2010**, *132*, 8538. Long, J.; Habib, F.; Lin, P.-H.; Korobkov, I.; Enright, G.; Ungur, L.; Wernsdorfer, W.; Chibotaru, L. F.; Murugesu, M. *J. Am. Chem. Soc.* **2011**, *133* (14), 5319.

(5) (a) Kajiwara, T.; Nakano, M.; Takaishi, S.; Yamashita, M. *Inorg. Chem.* **2008**, *47*, 8604. (b) Kajiwara, T.; Takahashi, K.; Hiraizumi, T.; Takaisi, S.; Yamashita, M. *CrystEngComm* **2009**, *11*, 2110 and references therein. (c) Costes, J. P.; Garcia-Tojal, J.; Tuchagues, J. P.; Vendier, L. *Eur. J. Inorg. Chem.* **2009**, 3801 and references therein. Costes, J. P.; Vendier, L. *Eur. J. Inorg. Chem.* **2010**, 2768 and references therein.

(6) (a) Chandrasekhar, V.; Pandian, B. M.; Boomishankar, R.; Steiner, A.; Vittal, J. J.; Houri, A.; Clérac, R. *Inorg. Chem.* **2008**, *47*, 4918 and references therein. (b) Yamaguchi, T.; Sunatsuki, Y.; Ishida, H.; Kojima, M.; Akashi, H.; Re, N.; Matsumoto, N.; Pochaba, A.; Mrozinski, J. *Inorg. Chem.* **2008**, *47*, 5736 and references therein. (c) Yamaguchi, T.; Costes, J. P.; Kishima, Y.; Kojima, M.; Sunatsuki, Y.; Bréfuel, N.; Tuchagues, J. P.; Vendier, L.; Wernsdorfer, W. *Inorg. Chem.* **2010**, *49*, 9125 and references therein.

(7) *Supernova CCD system, CrysAlisPro Software system*, Version 1.171.33.55; Oxford Diffraction Ltd.: Yarnton, U.K., 2007.

(8) Altomare, A.; Cascarano, G.; Giacovazzo, C.; Guagliardi, A.; Moliterni, A. G. G.; Burla, M. C.; Polidori, G.; Cavalli, M.; Spagna, R. *SIR97: package for structure solution by direct methods*; University of Bari: Bari, Italy, 1997.

(9) Sheldrick, G. M. *SHELX97: program for crystal structure refinement*; University of Göttingen: Göttingen, Germany, 1997.

(10) Llunell, M.; Casanova, D.; Cirera, J.; Bofill, J. M.; Alemany, P.; Alvarez, S.; Pinsky, M.; Avnir, D. *SHAPE*, v1.1b; University of Barcelona: Barcelona, Spain, 2005.

(11) Costes, J.-P.; Dahan, F.; Dupuis, A.; Laurent, J.-P. *Chem.—Eur. J.* **1998**, *4*, 1616.

(12) Kajiwara, T.; Nakano, M.; Takahashi, K.; Takaishi, S.; Yamashita, M. *Chem.—Eur. J.* **2011**, *17*, 196.

(13) (a) Cirera, J.; Ruiz, E. *C. R. Chim.* **2008**, *11*, 1227. (b) Costes, J. P.; Dahan, F.; A. Dupuis, A. *Inorg. Chem.* **2000**, *39*, 165.

(14) Cole, K. S.; Cole, R. H. *J. Chem. Soc.* **1941**, *9*, 341.